Japanese Journal of Applied Physics **51** (2012) 02BJ07 **REGULAR PAPER**
DOI: 10.1143/JJAP.51.02BJ07

Steady-State Solution for Dark States Using a Three-Level System in Coupled Quantum Dots

Tetsufumi Tanamoto*, Keiji Ono[1], and Franco Nori[2,3]

Corporate R&D center, Toshiba Corporation, Kawasaki 212-8582, Japan
[1]*Low Temperature Physics Laboratory, RIKEN, Wako, Saitama 351-0198, Japan*
[2]*Advanced Science Institute, RIKEN, Wako, Saitama 351-0198, Japan*
[3]*Physics Department, The University of Michigan, Ann Arbor, MI 48109-1040, U.S.A.*

Received September 26, 2011; accepted November 7, 2011; published online February 20, 2012

Quantum dots (QDs) are one of the promising candidates of interconnection between electromagnetic field and electrons in solid-state devices. Dark states appear as a result of coherence between the electromagnetic fields and the discrete energy levels of the system. Here, we theoretically solve the steady-state solutions of the density matrix equations for a thee-level double QD system and investigate the condition of the appearance of a dark state. We also numerically show the appearance of the dark state by time-dependent current characteristics.

1. Introduction

Future quantum communication systems might be composed of optical fiber networks and quantum computers based on solid-state qubits. Even though quantum computers made by optical systems would be smoothly connected to optical communication networks, in order to interface to mobile electronic systems, such as mobile phones, quantum computers based on solid-state circuits are desirable.[1–3)] In this respect, an efficient interconnection between optical and solid-state systems should be developed. Quantum dot (QD) systems, such as GaAs/AlGaAs[4–7)] have discrete energy levels which are suitable for the transfer of photon or phonon energies to electrons in solid-state circuits and can be used as elements of qubits.[8–12)] QD systems also have the advantage that the distance between energy-levels can be controlled by the bias, in addition to the sizes of the QDs. Thus QD systems are one of the promising candidates for the interconnection between optics and solid-state circuits.

One of the efficient connection methods is constructed by using coherent population trapping (CPT) or electromagnetically induced transparency (EIT).[13)] CPT is a typical phenomena of quantum coherence in three-level system and has been intensively studied in optics.[14–19)] By adjusting two laser fields, the electron population between the lowest two energy-levels are coherently transferred. Here, we theoretically discuss the interaction between an electromagnetic field and a coupled double QD (DQD) system by focusing on transport properties of three-level systems.

Recently CPT has been studied in superconducting qubit systems.[20–22)] Double quantum dot (DQD) systems such as GaAs/AlGaAs[4–6)] or Si/SiO_2 are also candidates for realizing three-level systems and have been theoretically investigated.[23,24)] Tokura *et al.*[12)] theoretically investigated resonant tunneling currents under locally different Zeeman energies and found that when the magnetic fields in each QD are non-collinear, four resonant peaks can be observed. Ke *et al.*[23)] constructed density matrix equations and investigates the relation between the phase of the driving lasers and transport properties. Emary *et al.*[24)] investigated transport properties when three-energy levels exist in the same QD. From an experimental viewpoint, applying two laser fields is not easy to control. Here, we mainly discuss the case where one of the laser fields can be replaced by electronic tunneling between two QDs.

*E-mail address: tetsufumi.tanamoto@toshiba.co.jp

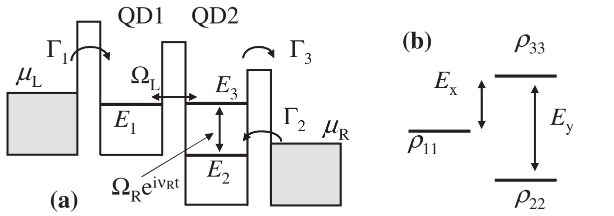

Fig. 1. (a) A three-level system in double QDs (DQDs). A bias voltage is applied between the left and right electrodes. (b) A density matrix for the three level. We define $E_x \equiv E_3 - E_1$ and the detuning $E_y \equiv E_3 - E_2 - \nu_R$. The dark state is a state with $\rho_{33} = 0$.

A three-energy-level DQD system is realized under a large bias voltage as depicted in Fig. 1, in which there is one energy-level (E_1) in the left QD and two (E_2 and E_3) in the right QD. We assume a strong Coulomb interaction between electrons such that only one excess electron is allowed in the two QDs. We also assume that the left energy level E_1 is close to the right upper energy level E_3 such that electrons in QD1 tunnel directly into E_3 ($E_3 - E_1 \ll \Omega_L$; and Ω_L is the tunneling rate between QD1 and QD2).

The dark state is a state in which there is no electron in the E_3 level and induces interesting phenomena in the transport properties of the DQD system. Let us first think about the case of conventional tunneling processes without the dark state: an electron tunnels from the left electrode to the QD1 with a tunneling rate Γ_1. When the laser pulse is switched off, the electron is trapped at the E_2 level with some probability. Once the electron is trapped at the E_2 level, because of the Coulomb blockade effect, there is no current through the DQD. When the laser pulse is switched on, the electron is excited from the E_2 level to the E_3 level. By the electron tunneling from the E_3 level to the right electrode, the current finally flows through the DQD. Then, the Coulomb blockade is released, and a new electron can tunnel from the left electrode to the QD1. Thus, as long as the laser pulse sequence continues, the current continues to flow. However, when the dark state is realized, the three-level system is in a coherent superposition state, and because there is no electron in the E_3 level, the current does not flow through the DQD system in spite of the applying laser field and bias voltage.

The purpose of this paper is to show the conditions for the production of a dark state, as functions of the Rabi frequency and the detuning parameter of the external laser field. We derive the density matrix equations in the three-level DQD system, and derive a steady-state solution for a dark state. We investigate the relationship between the time-dependent current characteristic and the dark state.

This article is organized as follows. In §2, the formulation of our model is presented. In §3, we show the analysis of the steady-state solution of the dark state. Section 4 is devoted to the numerical calculations for the time-dependent current when there is a dark state. The conclusions are given in §5. The detailed analytical solutions of the dark state in its steady state are shown in the Appendix. We also argue the analysis of the $\rho_{22} = 0$ state in the Appendix.

2. Formulation

The Hamiltonian is $H = H_0 + H_t + H_l + H_\gamma$, where

$$\begin{aligned} H_0 &= E_1|1\rangle\langle 1| + E_2|2\rangle\langle 2| + E_3|3\rangle\langle 3|, \\ H_t &= -(\Omega_L|1\rangle\langle 3| + \Omega_R e^{-i\nu_R t}|2\rangle\langle 3|) + \text{h.c.}, \\ H_l &= \sum_{\alpha=L,R}\sum_{k_\alpha} E_{k_\alpha}|k_\alpha\rangle\langle k_\alpha|, \\ H_\gamma &= \sum_{k_L} V_L|k_L\rangle\langle 1| + \sum_{k_R} V_R|k_R\rangle\langle 2| + \text{h.c.} \end{aligned} \tag{1}$$

Here $|i\rangle$ $(i = 1, 2, 3)$ is the energy-level in QDs, $|k_L\rangle$ ($|k_R\rangle$) is the left (right) electrode state. Ω_R is the Rabi frequency between E_2 and E_3, induced by an external laser field, and ν_R is the laser frequency. V_L (V_R) are the tunneling strengths of electrons between the left (right) electrode and the left (right) QD. The density matrix $\rho_{ij} \equiv |i\rangle\langle j|$ at $T = 0$ is derived using

$$\frac{d\rho}{dt} = -\frac{i}{\hbar}[H, \rho] - \frac{1}{2}\{\hat{\gamma}, \rho\}, \tag{2}$$

where $\hat{\gamma}$ expresses the dissipation of the system. In the present case of a QD system, the electron tunnelings between the QD and the electrodes correspond to this dissipation (hereafter we set $\hbar = 1$). When we define

$$\tilde{\rho}_{32} = \rho_{32}e^{i\nu_R t}, \tag{3}$$

$$\tilde{\rho}_{21} = \rho_{21}e^{-i\nu_R t}, \tag{4}$$

$$\tilde{\rho}_{31} = \rho_{31}, \tag{5}$$

$$\tilde{\rho}_{ii} = \rho_{ii}, \ (i = 1, 2, 3) \tag{6}$$

the density matrix equations are given by[23]

$$\begin{aligned} \frac{d\tilde{\rho}_{00}}{dt} &= \Gamma_1^{(h)}\tilde{\rho}_{11} + \Gamma_2^{(h)}\tilde{\rho}_{22} + \Gamma_3^{(h)}\tilde{\rho}_{33} \\ &\quad - (\Gamma_1^{(e)} + \Gamma_2^{(e)} + \Gamma_3^{(e)})\tilde{\rho}_{00}, \\ \frac{d\tilde{\rho}_{11}}{dt} &= \Gamma_1^{(e)}\tilde{\rho}_{00} - \Gamma_1^{(h)}\tilde{\rho}_{11} + i\Omega_L^*\tilde{\rho}_{31} - i\Omega_L\tilde{\rho}_{13} \\ &\quad + it_0(\tilde{\rho}_{12} - \tilde{\rho}_{21}), \\ \frac{d\tilde{\rho}_{22}}{dt} &= \Gamma_2^{(e)}\tilde{\rho}_{00} - \Gamma_2^{(h)}\tilde{\rho}_{22} + i\Omega_R^*\tilde{\rho}_{32} - i\Omega_R\tilde{\rho}_{23} \\ &\quad - it_0(\tilde{\rho}_{12} - \tilde{\rho}_{21}), \\ \frac{d\tilde{\rho}_{33}}{dt} &= \Gamma_3^{(e)}\tilde{\rho}_{00} - \Gamma_3^{(h)}\tilde{\rho}_{33} + i\Omega_L\tilde{\rho}_{13} - i\Omega_L^*\tilde{\rho}_{31} \\ &\quad + i\Omega_R\tilde{\rho}_{23} - i\Omega_R^*\tilde{\rho}_{32}, \\ \frac{d\tilde{\rho}_{31}}{dt} &= -(i\omega_{31} + \gamma_{31})\tilde{\rho}_{31} - i\Omega_L(\tilde{\rho}_{33} - \tilde{\rho}_{11}) \\ &\quad + i\Omega_R\tilde{\rho}_{21}, \\ \frac{d\tilde{\rho}_{32}}{dt} &= -[i(\omega_{32} - \nu_R) + \gamma_{32}]\tilde{\rho}_{32} \\ &\quad - i\Omega_R(\tilde{\rho}_{33} - \tilde{\rho}_{22}) + i\Omega_L\tilde{\rho}_{12}, \\ \frac{d\tilde{\rho}_{21}}{dt} &= -[i(\omega_{21} + \nu_R) + \gamma_{21}]\tilde{\rho}_{21} - i\Omega_L\tilde{\rho}_{23} + i\Omega_R^*\tilde{\rho}_{31} \\ &\quad - it_0(\tilde{\rho}_{11} - \tilde{\rho}_{22}), \end{aligned} \tag{7}$$

where γ_{31}, γ_{32}, and γ_{21} represent decoherence, such as acoustic phonons. In the present conditions, ρ_{i0} and ρ_{0i} are given by:

$$\frac{d\tilde{\rho}_i}{dt} = -i(\omega_{i0} + \gamma_{i0})\tilde{\rho}_{i0}. \tag{8}$$

These equations are solved analytically, but they are independent of the density matrix equations eq. (5), therefore, irrelevant to main transport properties; $\omega_{ij} \equiv E_i - E_j$ $(i = 1, 2, 3)$; Γ_i^e represents an electron tunneling from the DQD to the electrodes, and $\Gamma_i^{(h)}$ represents that from the electrodes to the DQD, where $\Gamma_i^{(x)} \equiv 2\pi\rho_i(E_{Fi})|V_i^{(x)}|^2$, with $\rho_\alpha(E_{Fi})$ $(i = 1, 2, 3$ and $x = \text{e, h})$, for each electrode at the Fermi energy E_{Fi} $(E_{F1} = \mu_L, E_{F2} = E_{F3} = \mu_R)$.

Depending on the relative positions of E_1, E_2 and E_3, we can classify the electron transport into the following two regions.

(1) $\Gamma_2^{(h)} = 0$ $(E_2 \gg \mu_R)$,
(2) $\Gamma_2^{(e)} = 0$ $(E_2 \ll \mu_R)$.

Because there is a finite bias between the left and right electrodes, the electron does not flow into E_3 from the eight electrodes, such that $\Gamma_1^{(h)} = 0$ and $\Gamma_3^{(e)} = 0$ are satisfied. In this paper we consider the case shown in Fig. 1 and set $\Gamma_2^{(e)} = 0$, $\Gamma_1^{(h)} = 0$, and $\Gamma_3^{(e)} = 0$ (this is the case in which a dark state explicitly exists). Hereafter we consider $\gamma_{31} = \gamma_0 = \gamma_{32}$.

3. Steady-State Solutions for the Dark State

Steady-state solutions are obtained from the density matrix equations when $d\rho_{ij}/dt = 0$. Compared with the optical three-level,[25] the existence of the ρ_{00} state complicates the equations. A dark state corresponds to the case where there is no electron state in E_3 as $\tilde{\rho}_{33} = 0$. For a given DQD, we can control the electron tunneling by adjusting the laser field (Ω_R and ν_R). When $t_0 = 0$, we can express the steady-state solution by fourth-order polynomial equations of E_x, E_y, and Ω_R, such as

$$\tilde{\rho}_{33} \propto A_{33}\left(\frac{\Omega_R}{\Omega_L}\right)^4 + B_{33}\left(\frac{\Omega_R}{\Omega_L}\right)^2 + C_{33} = 0, \tag{9}$$

where

$$A_{33} = \gamma_0'(-\Gamma_2' + \gamma_{21}'), \tag{10}$$

$$\begin{aligned} B_{33} &= -E_y'D_z'\Gamma_2'\gamma_{21}' + D_z^{2\prime}(\Gamma_2' + \gamma_0')\gamma_0' \\ &\quad + \gamma_{21}'\gamma_0' + \gamma_{21}^{2\prime}\gamma_0^{2\prime}, \end{aligned} \tag{11}$$

$$\begin{aligned} C_{33} &= \Gamma_2'\gamma_0'[(1 + D_z'E_y')^2 + \gamma_{21}^{2\prime}E_y^{2\prime} \\ &\quad + (D_z^{2\prime} + \gamma_{21}^{2\prime})\gamma_0^{2\prime} + 2\gamma_{21}'\gamma_0'], \end{aligned} \tag{12}$$

with $D_z \equiv E_x - E_y = E_2 - E_1 + \nu_R$ (all quantities are rescaled by Ω_L and indicated by the prime symbol, such

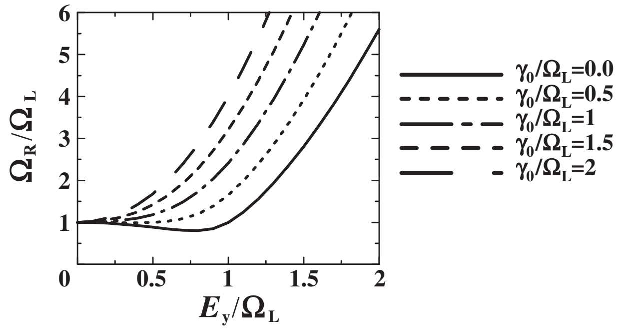

Fig. 2. The Rabi frequency Ω_R needed for realizing a dark state, as a function of the detuning E_y and γ_0. Here, $E_x = 0$, $\gamma_{21} = 0$, $t_0 = 0$, and $\Gamma_1 = \Gamma_2 = \Gamma_3$. These are solutions of $\rho_{33} = 0$ in eq. (9).

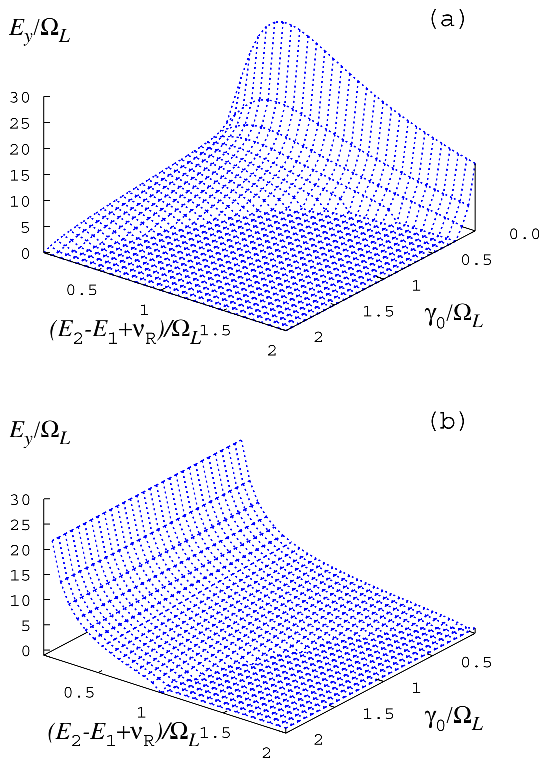

Fig. 3. (Color online) Condition of the dark state of E_y as functions of $E_2 - E_1 + \nu_R$ and γ_0 when (a) $\gamma_{21} = 0.5\Omega_L$ and (b) $\gamma_{21} = 0$. Equation (9) is solved for E_y. We take $t_0 = 0$, $\Omega_R = 2\Omega_L$ and $\Gamma_2 = \Omega_L$.

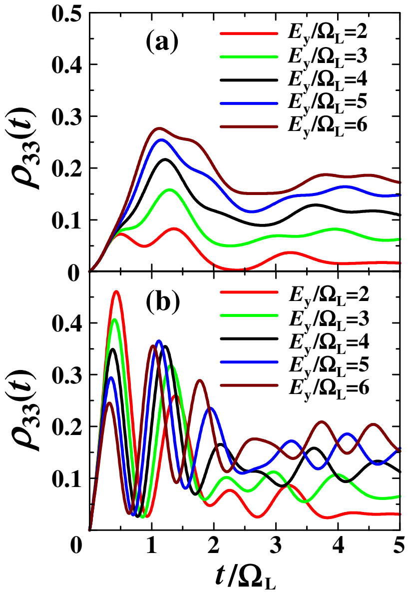

Fig. 4. (Color online) Time-dependent density matrix elements $\rho_{33}(t)$ starting from an initial state of (a) $|1\rangle$ and (b) $(|1\rangle + |2\rangle)/2$. Here, $\gamma_0/\Omega_L = 1$, $t_0 = 0$ and $\gamma_{21} = 0$. Also, $E_y/\Omega_L = 5$ corresponds to the solution of eq. (9).

as $\Gamma_2' = \Gamma_2/\Omega_L$). This equation is a parabolic function regarding Ω_R^2 with $C_{33} > 0$. Thus, if $\Gamma_2 > \gamma_{21}$, $\rho_{33}(\Omega_R^2) = 0$ has a solution for positive Ω_R^2. Also when $\Gamma_2 > \gamma_{21}$, the coefficient of Ω_R^4 has a negative value, therefore, the Ω_R^2 of eq. (9) for the dark state is a maximum value for the solutions of the density matrix equations to be valid. Figure 2 plots Ω_R, which satisfies $\rho_{33}(\Omega_R^2) = 0$ as a function of E_y/Ω_L. It can be seen that the larger Ω_R is required as E_y or decoherence γ_0 increases.

Equation (12) shows the relationship between E_y and $E_2 - E_1 + \nu_R$. Figure 3 show E_y as functions of $E_2 - E_1 + \nu_R$ and γ_0 for $\gamma_{21} = 0$, and $\gamma_{21} = 0.5\Omega_L$. We can see that the region of the existence of E_y for the dark state becomes smaller in particular when γ_{21} becomes larger. When $\gamma_{21} = 0$, E_y is given by

$$E_y = \frac{1}{D_x\sqrt{\Gamma_2}}\Big(-\sqrt{\Gamma_2} + \sqrt{\Gamma_2\Omega_R^4 - D_x^2(\Gamma_2 + \gamma_0)\Omega_R^2 - D_x^2\Gamma_2\gamma_0^2}\Big) \quad (13)$$

Because the equation in the root square in this equation should have a real solution, we have the condition:

$$E_2 - E_1 + \nu_R > \frac{2\Gamma_2\gamma_0}{2\Gamma_2 + \gamma_0}. \quad (14)$$

Thus, when the decoherence γ_0 is larger than the tunneling rate Γ, $E_2 - E_1 + \nu_R > 2\Gamma$, and when the decoherence γ_0 is smaller than the tunneling rate Γ, we have $E_2 - E_1 + \nu_R > \gamma_0$.

4. Time-Dependent Current

Here we show numerical results for the time-dependent matrix element ρ_{33} and current. Ω_R is calculated from eq. (9) such that the initial E_y is given, e.g., as $E_y/\Omega_L = 2$. Figure 4 shows the time-dependent density matrix element ρ_{33} when $E_x = 0$, $t_0 = 0$, and $\gamma_{21} = 0$, starting from (a) $|1\rangle$ and (b) $(|1\rangle + |2\rangle)/2$. It can be seen that, as E_y decreases, $\rho_{33}(t)$ decreases.

As mentioned above, Ω_R is determined such that it satisfies the steady-state solution $\rho_{33}(t \to \infty) \to 0$ for $E_y/\Omega_L = 2$, where $\rho_{33}(t \to \infty)$ has the lowest values. Compared with Fig. 4(a), Fig. 4(b) oscillates faster. This is because, for the superposition state, the density population of electrons oscillates between $|1\rangle$ and $|2\rangle$ more often than the case starting from $|1\rangle$.

Figure 5 shows the time-dependent currents through the DQD system. The current is derived[26] as

$$I(t) = \Gamma_R\big[\rho_{33}(t) + \rho_{22}(t)\big]. \quad (15)$$

Here we consider $\tilde{I}(t) \equiv e^{i\nu_R t}I(t)$. Ω_R is determined similarly to Fig. 4. Thus the current is expected to be reduced for

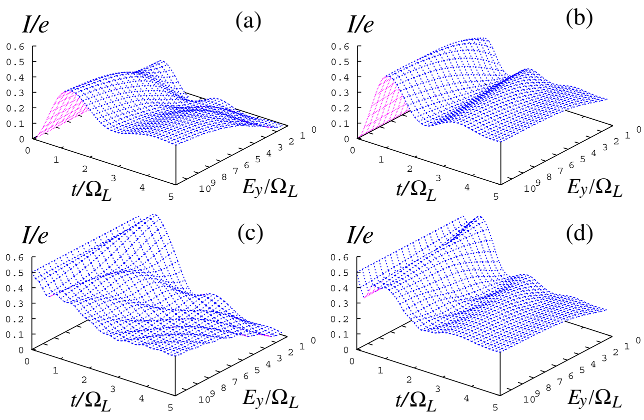

Fig. 5. (Color online) Time-dependent current as a function of E_y starting from $|1\rangle$ for (a) and (b), $(|1\rangle + |2\rangle)/2$ for (c) and (d). $\Gamma_1/\Omega_L = \Gamma_2/\Omega_L = \Gamma_3/\Omega_L = 1$, $\gamma_0/\Omega_L = 1$, (a, c) $t_0/\Omega_L = 0$ and $\gamma_{21}/\Omega_L = 0$. (b, d) $t_0/\Omega_L = 1$ and $\gamma_{21}/\Omega_L = 1$.

$E_y/\Omega_L = 2$. Figures 5(a) and 5(c) show that the current decreases around the expected dark state. Figures 5(c) and 5(d) show the time-dependent currents starting from a superposition state of $(|1\rangle + |2\rangle)/2$. Compared with Figs. 5(a) and 5(c), Figs. 5(b) and 5(d) show that a finite leak tunneling ($t_0 = 0.5$ and $\gamma_{21} = 0.5$) leads to a small current reduction, and the evidence of the dark state disappears regardless of the initial state.

5. Conclusions

We theoretically solved the steady-state solutions of the density matrix equations for a thee-level DQD system, and showed the condition for the appearance of a dark state. Numerical calculations for time-dependent current characteristics showed that the steady-state can be detected by measuring a current.

Acknowledgements

FN was partially supported by LPS, NSA, ARO, NSF grant No. 0726909, JSPS-RFBR contract No. 09-02-92114, Grant-in-Aid for Scientific Research S, Innovative Areas on Quantum Cybernetics from the Ministry of Education, Culture, Sports, Science and Technology, and the Japan Society for the Promotion of Science via its FIRST program. TT thanks A. Nishiyama, J. Koga, and S. Fujita for useful discussions.

Appendix A: Explicit Form of Density Matrix

Because the equations for $t_0 = 0$ are still too complicated, we describe the case of $E_x = 0$.

$$\begin{aligned}\rho_{11} = \frac{\Gamma'}{Z_0}&\{\gamma_0'\Omega_R^{2\prime}((E_y^{2\prime} + \gamma_{21}^{2\prime})\gamma_0'(1+\Gamma'\gamma_0') \\ &+ \Gamma'\Omega_R^{2\prime}(1+\Omega_R^{2\prime}) + \gamma_{21}'[1+\Omega_R^{2\prime} + \Gamma'\gamma_0'(1+2\Omega_R^{2\prime})]) \\ &+ \Gamma_2'(\Gamma'(E_y^{2\prime}+\gamma_{21}^{2\prime})\gamma_0^{4\prime} \\ &+ [E_y^{2\prime} + \gamma_{21}'(2\Gamma'+\gamma_{21}')]\gamma_0^{3\prime}(1+\Omega_R^{2\prime}) \\ &+ E_y^{2\prime}\Omega_R^{2\prime}(\gamma_{21}' + \Gamma'\Omega_R^{2\prime}) \\ &+ \gamma_0'[E_y^{4\prime} + (-1+\Omega_R^{2\prime})^2(1+\Omega_R^{2\prime}) \\ &+ E_y^{2\prime}(-2+\gamma_{21}^{2\prime} + 2\Omega_R^{2\prime} + 2\Gamma'\gamma_{21}'\Omega_R^{2\prime})] \\ &+ \gamma_0^{2\prime}[2\gamma_{21}'(1+\Omega_R^{4\prime}) + \Gamma' h_2])\}, \end{aligned} \quad (A\cdot1)$$

$$\rho_{22} = \frac{\Gamma'\gamma_0'\Omega_R^{2\prime}}{Z_0}[h_1 + \Gamma'(1 - E_y^{2\prime} + \gamma_{21}'\gamma_0' + \Omega_R^{2\prime})], \quad (A\cdot2)$$

$$\begin{aligned}\rho_{33} = \frac{\Gamma'}{Z_0}&\{\gamma_0'\Omega_R^{2\prime}h_1 + \Gamma_2'(2\gamma_{21}'\gamma_0^{2\prime} + (E_y^{2\prime} + \gamma_{21}^{2\prime})\gamma_0^{3\prime} \\ &+ E_y^{2\prime}\gamma_{21}'\Omega_R^{2\prime} + \gamma_0'[1 + E_y^{4\prime} - \Omega_R^{4\prime} \\ &+ E_y^{2\prime}(-2+\gamma_{21}^{2\prime} + \Omega_R^{2\prime})])\}, \end{aligned} \quad (A\cdot3)$$

$$\begin{aligned}Z_0 = \Gamma^{2\prime}&[\gamma_0'\Omega_R^{2\prime}(E_y^{2\prime}(-1+\gamma_0^{2\prime}) + (1+\gamma_{21}'\gamma_0' + \Omega_R^{2\prime})^2) \\ &+ \Gamma_2'\gamma_0'\Omega_R^{2\prime}h_1 + \Gamma_2'[(E_y^{2\prime}+\gamma_{21}^{2\prime})\gamma_0^{4\prime} \\ &+ 2E_y^{2\prime}\gamma_{21}'\gamma_0'\Omega_R^{2\prime} \\ &+ E_y^{2\prime}\Omega_R^{4\prime} + 2\gamma_{21}'\gamma_0^{3\prime}(1+\Omega_R^{2\prime}) + \gamma_0^{2\prime}h_2)], \\ &+ \Gamma'[4\gamma_0'\Omega_R^{2\prime}h_1 + \Gamma_2'(3E_y^{2\prime}\gamma_{21}'\Omega_R^{2\prime} \\ &+ \gamma_0^{3\prime}(E_y^{2\prime}+\gamma_{21}^{2\prime})(3+\Omega_R^{2\prime}) \\ &+ \gamma_{21}'\gamma_0^{2\prime}(6+\Omega_R^{2\prime}+2\Omega_R^{4\prime}) + \gamma_0'(3+3E_y^{4\prime} - 2\Omega_R^{4\prime} \\ &+ \Omega_R^{6\prime} + 3E_y^{2\prime}(-2+\gamma_{21}^{2\prime}+\Omega_R^{2\prime})))], \end{aligned} \quad (A\cdot4)$$

where

$$h_1 = (E_y^{2\prime} + \gamma_{21}^{2\prime})\gamma_0' + \gamma_{21}'(1+\Omega_R^{2\prime}), \quad (A\cdot5)$$

$$h_2 = E_y^{4\prime} + E_y^{2\prime}(-2+\gamma_{21}^{2\prime}) + (1+\Omega_R^{2\prime})^2. \quad (A\cdot6)$$

Here, all quantities are scaled by Ω_L such as $\Omega_R' = \Omega_R/\Omega_L$, $\Gamma' = \Gamma/\Omega_L$ and so on.

Appendix B: $\rho_{22} = 0$ State

In the main text, we discussed the dark state condition of $\rho_{33} = 0$. Here, we consider the region of $\rho_{22} = 0$ without considering the dark state. Because there is no direct tunneling term between the E_1 level and the E_2 level, an electron exists at the energy-level E_2 only when there is some relaxation process of the electron from the E_3 level or dissipation. If the electron is transferred from the left electrode to the right electrode without the E_2 level, we can regard the system as a two-level system as if each QD has one energy-level. The condition $\rho_{22} = 0$ corresponds to:

$$\begin{aligned}\rho_{22} \propto &-\gamma_0(\Gamma-\gamma_0)(E_x^2+E_y^2) \\ &+ [2\gamma_0(\Gamma-\gamma_0) + \Gamma\gamma_{21}]E_xE_y \\ &+ \gamma_0(\gamma_{21}+\Gamma)[\Omega_L^2 + \gamma_{21}\gamma_0 + \Omega_R^2] = 0 \end{aligned} \quad (B\cdot1)$$

Thus, E_y is written as function of E_x:

$$E_y = \frac{1}{a_2}\left[b_2E_x + \sqrt{(b_2^2 - 4a_2^2)E_x^2 + 4a_2c_2}\right] \quad (B\cdot2)$$

where

$$a_2 = \gamma_0(\Gamma-\gamma_0) \quad (B\cdot3)$$

$$b_2 = a_2 + \Gamma\gamma_{21} \quad (B\cdot4)$$

$$c_2 = \gamma_0(\gamma_{21}+\Gamma)[\Omega_L^2 + \gamma_{21}\gamma_0 + \Omega_R^2]. \quad (B\cdot5)$$

This is the condition that the present system can be treated as a two-level system. When $\gamma_{21} = 0$, we can simplify the condition as

$$E_y = E_x + \sqrt{\frac{\Gamma(\Omega_L^2+\Omega_R^2)}{\Gamma-\gamma_0}}. \quad (B\cdot6)$$

1) J. Q. You and F. Nori: Nature **474** (2011) 589.
2) J. Q. You and F. Nori: Phys. Today **58** [11] (2005) 42.
3) A. V. Rozhkov, G. Giavaras, Y. P. Bliokh, V. Freilikher, and F. Nori: Phys. Rep. **503** (2011) 77.
4) K. Ono and S. Tarucha: Phys. Rev. Lett. **92** (2004) 256803.
5) W. G. van der Wiel, T. Fujisawa, S. Tarucha, and L. P. Kouwenhoven: Jpn. J. Appl. Phys. **40** (2001) 2100.
6) R. Takahashi, K. Kono, S. Tarucha, and K. Ono: Jpn. J. Appl. Phys. **50** (2011) 04DJ03.
7) R. Takahashi, K. Kono, S. Tarucha, and K. Ono: Jpn. J. Appl. Phys. **49** (2010) 04DJ07.
8) T. Tanamoto: Phys. Rev. A **61** (2000) 022305.
9) T. Tanamoto: Jpn. J. Appl. Phys. **49** (2010) 04DJ08.
10) T. Tanamoto and K. Muraoka: Appl. Phys. Lett. **96** (2010) 022105.
11) Y. Hada and M. Eto: Jpn. J. Appl. Phys. **43** (2004) 7329.
12) Y. Tokura, T. Kubo, Y. S. Shin, K. Ono, and S. Tarucha: Physica E **42** (2010) 994.
13) T. Tanamoto and K. Ichimura: published unexamined patent application P2001-168353.
14) S. E. Harris: Phys. Today **50** [7] (1997) 36.
15) M. Fleischhauer, A. Imamoglu, and J. P. Marangos: Rev. Mod. Phys. **77** (2005) 633.
16) H. Sawamura, K. Toyoda, and S. Urabe: Jpn. J. Appl. Phys. **46** (2007) 1713.
17) H. Ian, Y. X. Liu, and F. Nori: Phys. Rev. A **81** (2010) 063823.
18) Z. Z. Li, S. H. Ouyang, C. H. Lam, and J. Q. You: EPL **95** (2011) 40003.
19) S. Debald, T. Brandes, and B. Kramer: Phys. Rev. B **66** (2002) 041301(R).
20) W. R. Kelly, Z. Dutton, J. Schlafer, B. Mookerji, and T. A. Ohki: Phys. Rev. Lett. **104** (2010) 163601.
21) W. Chua, S. Duan, and J. L. Zhua: Appl. Phys. Lett. **90** (2007) 222102.
22) F. Nori: Nat. Phys. **4** (2008) 589.
23) S. S. Ke and G. X. Li: J. Phys.: Condens. Matter **20** (2008) 175224.
24) C. Emary, C. Poltl, and T. Brandes: Phys. Rev. B **80** (2009) 235321.
25) R. G. Brewer and E. L. Hahn: Phys. Rev. A **11** (1975) 1641.
26) T. Tanamoto and X. Hu: Phys. Rev. B **69** (2004) 115301.